

# Precision Agriculture – Comparison and Evaluation of Innovative Very High Resolution (UAV) and LandSat Data

Antonis Kavvadias<sup>1</sup>, Emmanouil Psomiadis<sup>2</sup>, Maroulio Chanioti<sup>3</sup>, Eleni Gala<sup>1</sup>,  
Spyros Michas<sup>1</sup>

<sup>1</sup>En Agris LLC, Evias 3 15125, Maroussi, Greece, e-mail: info@enagris.gr

<sup>2</sup>Agricultural University of Athens, Laboratory of Mineralogy & Geology, Iera Odos 75, 118  
55, Athens, Greece, e-mail: mpsomiadis@aua.gr

<sup>3</sup>Inforest Research o.c, Glaraki 10B, 11145, Athens, Greece, e-mail: mchanioti@inforest.gr

**Abstract.** The Precision Agriculture primarily involves the use of geospatial technology to map the spatial changes in plant and soil conditions of crops and their correlation with agricultural inputs such as water, fertilizer, etc., at a spatial basis. For the present study, the UAV eBee of SenseFly SA was used, in order to demonstrate the utility and effectiveness of these new airborne instruments in the observation of crops. Also, the corresponding free data of the satellite Landsat-8 was used for the comparison. As study area the crop fields of the Agricultural University of Athens in Aliartos, Viotia were chosen. The NDVI (Normalized Difference Vegetation Index) given from the UAV and the Satellite was calculated separately by two different Softwares. A comparison and evaluation of the indicators of the two Remote Sensing means carried out, in order to examine the effectiveness of the data received from the UAV camera.

**Keywords:** Precision Agriculture, UAV, LandSat-8, NDVI

## 1 Introduction

A few years ago the use of UAVs was not that widespread. In the last decade, however, there was a rapid evolution of technology led to the creation of more sophisticated UAVs. The improved cameras that can carry, offer information in the Visible, Near-Infrared and Thermal part of the electromagnetic spectrum and the improved software of processing of images have led to the increasing use of the UAVs in Precision Agriculture (Xiang & Tian 2011, Mesas-Carrascosa et al. 2014, Torres-Sánchez et al. 2014, Rokhmana 2015).

In this study the UAV eBee of SenseFly SA and the camera Canon S110 NIR were used. The Canon S110 NIR takes images in Visible-Green, Visible-Red and Near-Infrared part of the electromagnetic spectrum.

---

Copyright © 2015 for this paper by its authors. Copying permitted for private and academic purposes.

Proceedings of the 7th International Conference on Information and Communication Technologies in Agriculture, Food and Environment (HAICTA 2015), Kavala, Greece, 17-20 September, 2015.

As study area was chosen the area of Aliartos, which belongs to the Agricultural University of Athens and includes an agricultural land of 110 hectares, with wheats, oats, alfalfa and fallow or uncultivated land (Figure 1).

Also, the choice of OLI receiver data was performed because the Landsat satellite system constitutes one of the most tested, designed and reliable satellite systems, even though the spatial resolution of 30m which provides is not fully considered satisfactory for pixel to pixel comparison with the UAV sensor. Therefore an attempt was made to compare the tendency of change of important vegetation indices such as NDVI. The two recording systems of the Landsat-8 satellite and the UAV provide recordings in the red and near infrared range of the electromagnetic radiation so that it is possible to calculate the NDVI index.



**Fig. 1.** The crops of the Agricultural University of Athens in Aliartos, Viotia, Greece Google Earth image

## 2 Data

### Normalized Difference Vegetation Index (NDVI)

Estimation of:

- General plant health condition
- Photosynthetic activity
- Possible deficiency of nutrients

$$NDVI = \frac{(NIR - Red)}{(NIR + Red)} \quad (1)$$

## 2.1 Satellite Images: Landsat-8 (OLI)

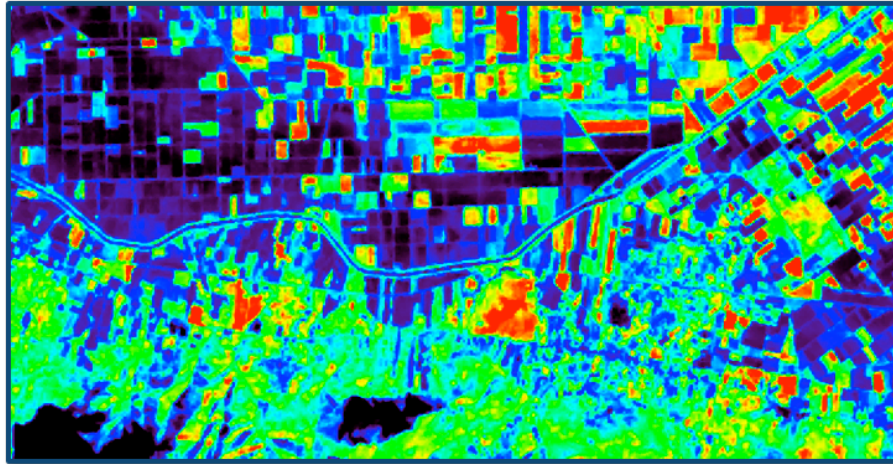


Fig. 2. Landsat-8 image of NDVI, Aliartos, 14/01/2015

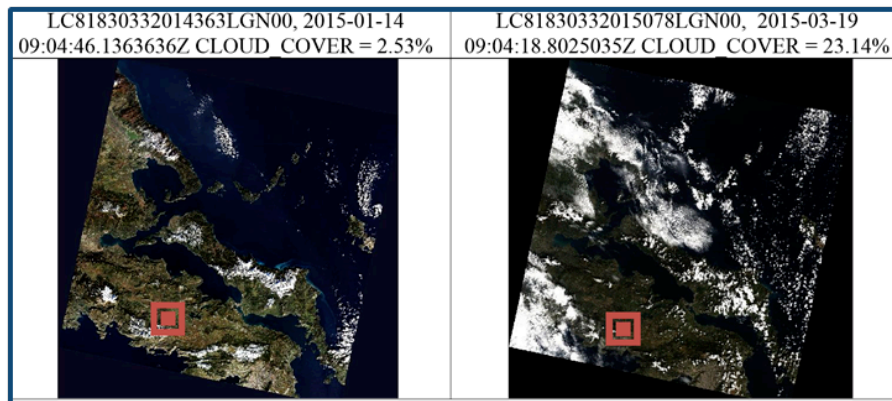


Fig. 3. The quicklooks of the Satellite images of Landsat-8 that were used

Table 1. The spectral bands of LandSat-8 that were used

Band	Wave Length (micrometers)	Resolution (meters)
Band 4 – Red	0.64 - 0.67	30
Band 5 - Near Infrared (NIR)	0.85 - 0.88	30
Band 8 – Panchromatic	0.50 - 0.68	15

## 2.2 UAV Images: EBee (Canon S110 NIR)

**Platform: eBee**

Gross Weight: 0.69 Kg

Wingspan: 96 cm

Max Flight Time: 45 min

Radio Link Range: 3 Km



**Fig. 4.** UAV Ebee

**Sensor: Canon S110 NIR**

Resolution: 12 MPixel

Bands:

- Green (G)
- Red (R)
- Near-infrared (NIR)

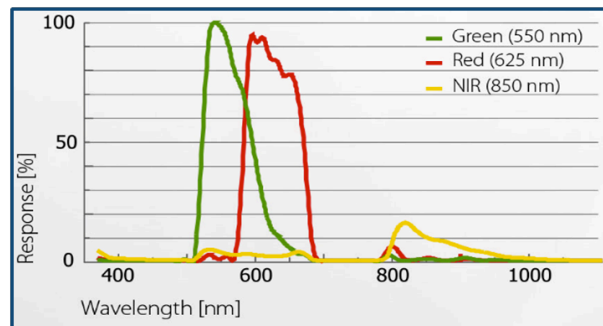


**Fig. 5.** The spectral ranges that the sensor Canon S110 NIR covers





**Fig. 6.** Wheat and Alfalfa crops, Aliartos. NIR image sample of eBee (Canon S110 NIR)

### **3 Methods**

#### **3.1 Landsat-8**

- **Geometric Correction**
- **Atmospheric Correction** (ENVI, version 5.2)
  - Top of Atmosphere reflectance (ToA Reflectance)
- Reflectance in the atmosphere
  - FLAASH (Fast Line-of-sight Atmospheric Analysis of Spectral Hypercubes)
- Reflectance on the ground
  - **Panchromatic sharpening**  
(NNDiffuse PanSharpening, ENVI)
    - Panchromatic (Res: 15m)
    - Spectral Bands (Res: 30m → 15m)
  - **NDVI export** (Res: 15m) (Fig. 7)



**Fig. 7.** Geometrically and Atmospherically corrected Landsat-8 image (Grayscale). Aliartos, 14/01/2015

### 3.2 UAV eBee

- **Flight Plans** (eMotion, SenseFly)
  - Image Resolution: 11cm/px
  - Lateral Overlap: 65%
  - Longitudinal Overlap: 80%

#### **Flights**

- Flight Duration: 25'
- Flight Height: 315m

#### **Image Post-process** (PostflightTerra 3D, Pix4D)

- Orthomosaic production
- Reflectance Map production
- NDVI map production



**Fig. 8.** UAV flight control monitor

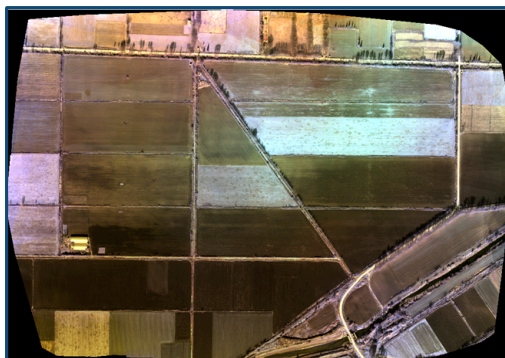


Fig. 9. Reflectance map of eBee. Aliartos, 14/01/2015

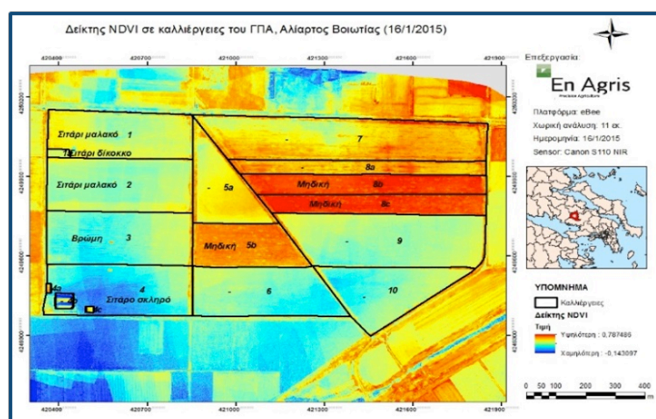


Fig. 10. NDVI Orthomosaic. Aliartos, 14/01/2015. Platform: eBee

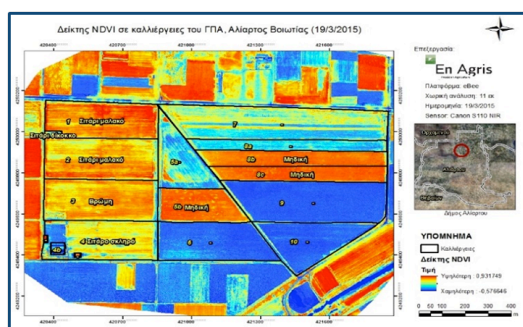


Fig. 11. NDVI Orthomosaic. Aliartos, 19/03/2015. Platform: eBee

## 4 Results – Discussion

The comparison of the NDVI values provided for the two periods (January and March) for each observation instrument (eBee and Landsat-8) carried out. Therefore we created a fishnet of values in such a way as to include any type of crop field. So the points 1-2-5 were selected in bare ground, the points 0-3-6 in fields that were sown in January and were grown in March (Soft wheat, Durum wheat and oats) and the points 4-7-8 in fields with different vegetation growth in each period (Alfalfa).

The NDVI values of the images were exported and reflected in a diagram for each period to a comparison of the trend of values for each observation instrument (Figure 13a and 13b). The comparison of the values in the diagrams showed a very good identification of the distribution (tendency) of the values for the two means of observation in both periods. Small deviations in some points, such as at point 0 in the diagram of January, are possibly due to the difference of spatial resolution between the images.

Also, in order to verify the given identification of the NDVI values between the two means of observation, a spatial profile of a linear section was created (Figure 14), so as to include, as many as possible different forms of vegetation; from bare soil to fields covered by full vegetation. The comparison of spatial profiles gave the same results to the charts and confirmed the very good identification of the distribution (tendency) of the values of the two means of observation in both periods (Figure 15).

### 4.1 Comparison of the tendency of NDVI values of the eBee & Landsat-8 for 14/01/2015 & 19/03/2015

#### 4.1.1 Fishnet creation (0-8)

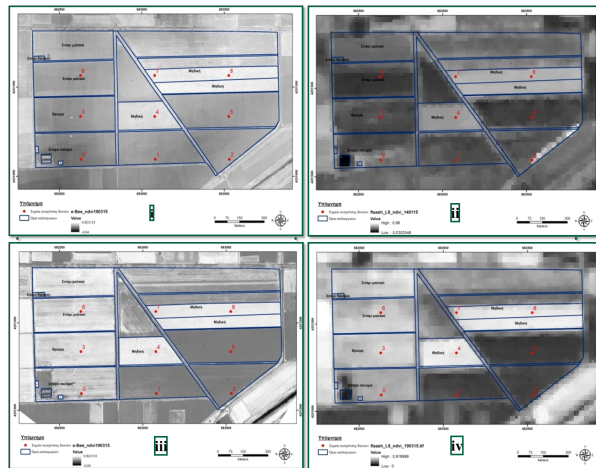


**Fig. 12.** The fishnet of selected points in the 4 maps; (i) eBee - January, (ii) Landsat\_8 - January, (iii) eBee - March, and (iv) Landsat\_8 - March

**Table 2.** The spectral bands of LandSat-8 that were used

Point	Cultivation
0	Durum Wheat
1	Bare Soil
2	Bare Soil
3	Oats
4	Alfalfa
5	Bare Soil
6	Soft Wheat
7	Alfalfa
8	Alfalfa

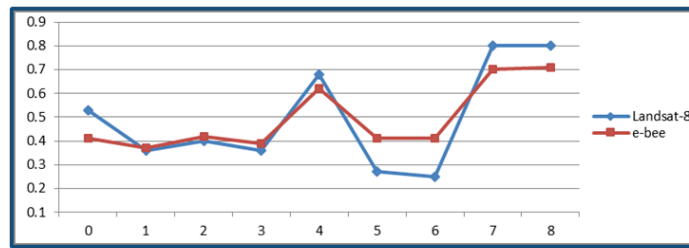


**Fig. 13a.** The NDVI values distribution of January, for the two means of observation

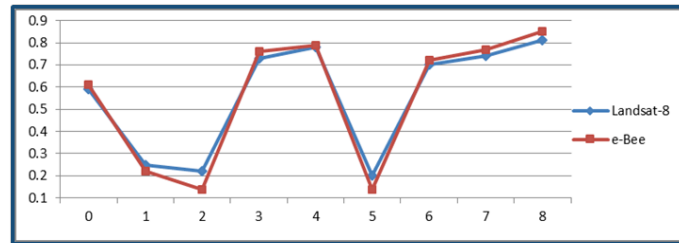


**Fig. 13b.** The NDVI values distribution of March, for the two means of observation

#### 4.1.2 Linear section creation and spatial profile production for the NDVI maps

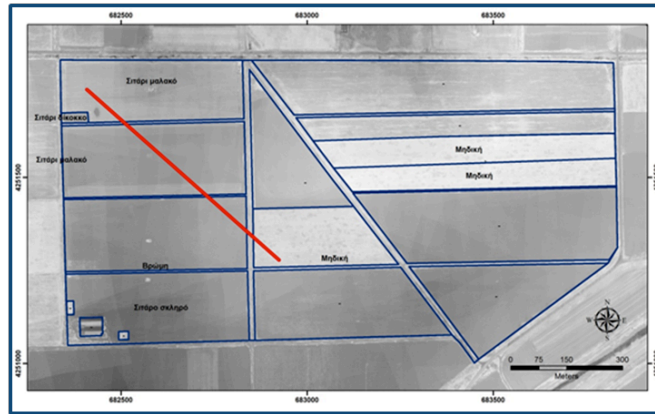


**Fig. 14.** The linear section (red line) that was chosen to create the spatial profile of the NDVI maps.

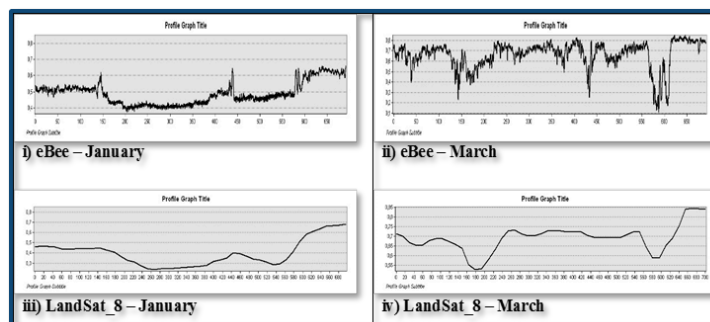


**Fig. 15.** The spatial profile of the linear section for the eBee (i, ii) and Landsat-8 (iii, iv) images for the January and March

## 5 Conclusion

The results of comparing the NDVI values of the two earth observation data have shown that there is a fairly good coincidence of the value variation between them, which demonstrates the excellent quality of the UAV data, while highlighting the usefulness for wider and more systematic use in Precision Agriculture. The UAVs as they offer a better spatial and temporal resolution, a higher speed and a lower cost, may offer more direct and easier solutions in agricultural production. Of course it is necessary and is a goal of further consideration in the near future, the comparison of the UAV with a remote sensing observational mean of a similar spatial resolution as well.



## References

1. Blackmore, S., 1994. Precision Farming; an introduction, Outlook on Agriculture, Vol. 23, No 4, 275-280.
2. Blackmore, S., H.W. Griepentrog, S.M. Pedersen, and S. Fountas, 2006. Precision Farming in Europe. In «Handbook of Precision Agriculture: Principles and Applications», The Haworth Press Inc., USA, 567-614.
3. El Nahry, A.H., Ali R.R., El Baroudy A.A., 2011. An approach for precision farming under pivot irrigation system using remote sensing and GIS techniques. Agricultural Water Management, Volume 98, Issue 4, 517-531.
4. Li, F., Mistele B., Hu Y., Chen X., Schmidhalter U., 2014. Optimising three-band spectral indices to assess aerial N concentration, N uptake and aboveground biomass of winter wheat remotely in China and Germany. ISPRS Journal of Photogrammetry and Remote Sensing, Volume 92, 112-123.
5. Mesas-Carrascosa, F. J., Notario-García, M.D., Meroño de Larriva, J.E., Sánchez de la Orden, M., García-Ferrer Porras, A., 2014. Validation of measurements of land plot area using UAV imagery, International Journal of Applied Earth Observation and Geoinformation, Vol. 33, 270-279.
6. Mulla, D., 2013. Twenty five years of remote sensing in precision agriculture: Key advances and remaining knowledge gaps. Biosystem Engineering, 114, 358-371.
7. Parente, C., 2013. TOA reflectance and NDVI calculation for Landsat 7 ETM+ images of Sicil. Department of Sciences and Technologies University of Naples “Parthenope”, Italy - The 2nd Electronic International Interdisciplinary Conference, 351 – 354.
8. Rokhmana, C. A., 2015. The Potential of UAV-based Remote Sensing for Supporting Precision Agriculture in Indonesia, Proc. Environmental Sciences, Vol. 24, 245-253.
9. Seelan, S.K., Laguette, S., Casady, G.M., Seielstad, G.A., 2003. Remote sensing applications for precision agriculture: A learning community approach. Remote Sensing of Environment, 88, 157-169.
10. Sun, W., Chen, B., Messinger, D.W., 2014. Nearest neighbor diffusion based pan-sharpening algorithm for spectral images. Optical Engineering, 53, no 1.
11. Torres-Sánchez, J., Peña, J.M., de Castro, A.I., López-Granados, F., 2014. Multi-temporal mapping of the vegetation fraction in early-season wheat fields using images from UAV. Computers and Electronics in Agriculture, Vol. 103, 104-113.
12. Xiang, H., Tian, L., 2011. Development of a low-cost agriculture remote sensing system based on an autonomous unmanned aerial vehicle (UAV). Biosystems Engineering, 108, 174-190.
13. Karydas, Ch. G., Syllaios, N. G., 2000. Precision Agriculture: Description of the method - Current state and prospects. 2<sup>nd</sup> Special Conference on Information Systems in Georgia, Chania, October 2000, 2, 8. (*in Greek*)